

The Effect of Boundary Layer Thickness on Cavity Flow over a Backward-Facing Step

B. W. Pearce, P. A. Brandner, S. Foster and G. A. Zarruk

Australian Maritime College
University of Tasmania, Launceston, Tasmania 7250, Australia

Abstract

Ventilated cavities detaching from a backward facing step are investigated for a range of upstream boundary layer thicknesses in a cavitation tunnel. The upstream turbulent boundary layer thickness is varied by artificial thickening of the test section natural boundary layer using an array of transversely injected jets. Momentum thickness Reynolds numbers from 8.5 to 28×10^3 were tested giving boundary layer thickness to step height ratios from 1.25 to 3.8. A range of cavitation numbers (based on the cavity pressure) were obtained by variation of the ventilation flow rate for fixed freestream Reynolds and cavitation numbers. Cavity length to step height ratios from 15 to 60 were achieved. Cavity length was found to be linearly dependent on ventilation rate and to decrease with increasing boundary layer thickness. This result may have implications in the practical optimization of these flows which occur in applications such as drag reduction on marine hull forms.

Introduction

A significant portion of the propulsive power requirements for a marine vessel, up to around 60%, is required to overcome the frictional drag due to the wetted surface area. Various techniques/devices have been incorporated into the design of ship hull forms in the endeavor to minimise this sizeable component of the total resistance. In the high-speed vessel sector, semi-displacement through to planning hull forms have been developed which are designed to augment the hydrostatic support with a component of hydrodynamic lift, i.e. generated due to vessel speed, resulting in a reduced wetted surface area and hence a reduction in frictional drag. The extreme of this concept is to lift the hull completely out of the water by means of hydrofoils or by air-cushion support [9]. For slower displacement hull forms there has been more recent interest in the modification of the near-hull flow field, e.g. by the addition of air bubbles/air layer [6, 8] or polymer solutions [14, 7], to reduce viscous hull resistance.

A subset within the broader air bubble/air layer drag reduction field is the formation of air filled cavities from backward-facing steps (BFS) in the hull. Developmental trials and basic studies have used air cavities covering 30 to 50% of the wetted hull surface [10, 15]. The inclusion of such a geometric discontinuity involves significant structural modification to the hull design resulting in a more complicated and expensive initial build. This added cost may be more than offset by net energy savings which in recent studies are reported to be in the order of 10 to 20% for large full displacement type vessels [11]. An aspect of these BFS cavity flows which has not been considered in the previous studies is the effect of the upstream turbulent boundary layer on the cavity physics. If significant, it may influence the efficiency of the drag reduction system and inform the optimal longitudinal location of the BFS, which determines the boundary layer thickness of the flow at the point of cavity detachment. The present work reports on an experimental investigation on the effect that an upstream boundary layer has on the geometry of a ventilated cavity forming from a BFS. A sketch of the basic flow investigated is shown in Figure 1 including notation of the

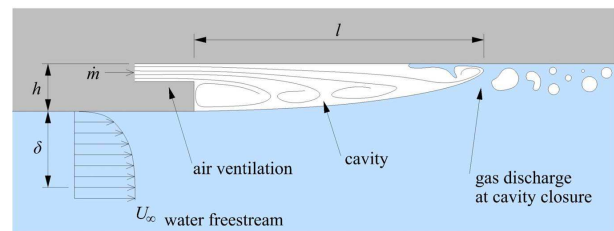


Figure 1. Sketch of a ventilated cavity detaching from a BFS with important flow features and parameters noted. Cavity length is measured from the step face to the closure of the main cavity structure. The ventilation air supply is admitted through the face adjacent to the face/downstream wall junction.

main flow features and parameters of interest.

Experimental Overview

CRL Water Tunnel

Experiments were carried out in the Cavitation Research Laboratory (CRL) water tunnel at the University of Tasmania. The tunnel test section is 2.6 m long, 0.6 m square at entrance and 0.6 m wide by 0.62 m deep at exit. The test section ceiling is horizontal with the floor sloping 20 mm to nominally maintain constant speed and zero streamwise pressure gradient. The operating velocity and pressure ranges are 2 to 12 m/s and 4 to 400 kPa absolute respectively. The tunnel volume is 365 m³ with demineralised water (conductivity of order 1 μ S/cm). The tunnel has ancillary systems for rapid degassing and for continuous injection and removal of nuclei and large volumes of incompressible gas. A detailed description of the facility is given in [3, 2]. Detailed specifications for the associated instrumentation can be found in [13].

Boundary Layer Thickening

The CRL water tunnel was developed with a capability to artificially thicken (or thin) the test section ceiling boundary layer of up to nominally 0.1 m thickness within the test section length. These thickened boundary layer profiles being close approximations to flat plate, zero pressure gradient, high Reynolds number turbulent boundary layers [1].

The boundary layer control system consists of an ancillary pipe circuit in parallel with the main tunnel circuit containing a pump and valves that enable the circuit to be configured for thickening or thinning of the test section ceiling boundary layer. Water is injected or ingested through a 0.6 m (spanwise) by 0.125 m, streamwise) penetration the trailing edge of which is located 0.115 m upstream of the test section entrance. The penetration may be fitted with a blank plate flush with the tunnel ceiling when not being used or with plates with nozzles, for either injection or suction, of various geometries as desired. Water is injected or ingested through the plate via a plenum in which the static pressure may be measured and compared with the tunnel dynamic pressure for real-time control. The plenum is connected to the ancillary circuit via a wide angle vaned diffuser

and two honeycombs.

The plate used for both thinning and thickening in this study is machined with an array of 252×5 mm diameter holes on a 16.8 mm triangular grid (8 spanwise rows). The plate is 15 mm thick and the holes have a 5 mm radius bellmouth entry. For thinning, ingested flow is returned to the main circuit at the downstream tank used for separation of large bubbles. For thickening, water is taken from the main circuit lower limb, where the flow is slow and has had any bubbles removed.

Experimental Setup

A 2-D plate (750 mm \times 10 mm) with a ‘quarter’ ellipse (5:1) leading edge was attached to the test section ceiling. Based on data from a previous study [4], the plate length was chosen to reduce the likelihood of leading edge perturbations affecting the cavity and the plate thickness, i.e. the height of the BFS, was chosen to be sufficient to minimise the likelihood of surface tension effects causing the cavity surface to contact with the wall. Compressed air is supplied through the tunnel wall into an internal manifold within the rear section of the plate from which air is admitted into the separation zone downstream of the BFS via an array of 1.6×1.6 mm nozzles at 15 mm spacing. The internal manifold reduces in section linearly from the center-line outwards to achieve a nominally constant discharge of air across the width of the plate. The air flow rate is measured and controlled using an Alicat Scientific model MCR-500-SLPM-D (0-500 Standard Liters per Minute (SLPM)) mass flow meter with an estimated precision of 3 SLPM.

The boundary layer profiles were measured on the test section vertical center plane, 50 mm upstream from the end of the plate, using a 0.7 mm outside, by 0.4 mm inside, diameter total head tube. A 1 mm diameter wall reference static tapping was located in line with the probe tip offset 50 mm from the centre plane. Boundary layer traverses consisted of 40 measurements on a log distribution. All measurements were taken at 1024 Hz sampling rate for durations corresponding to at least 5000 boundary layer turnover times (TU_∞/δ), where T is the measurement duration, U_∞ the freestream velocity and δ is the boundary layer thickness corresponding to 99% of freestream velocity [1]. All boundary layer measurements were taken in single phase flow conditions, i.e. without the ventilated cavity present, as otherwise the probe stem itself would have been susceptible to cavitation and a wake from the probe would have been present. This allowed for the ventilated air passage to be used also for the pitot tube with the hole in the plate plugged prior to the cavity measurements.

Images of the cavity were taken from below using a Canon EOS 50D SLR camera with a Canon EF24-70 mm zoom lens. The camera exposure was controlled using a triggered stroboscopic flash (Drello 1018/LE4040).

The cavity pressure was obtained from a tapping in the test section ceiling 30 mm downstream from the BFS. The pressure was measured via a gas liquid interface, placed at the test section ceiling height, a Validyne DP15TL differential pressure transducer (estimated precision of 0.2 kPa) via a Swagelok SS-43Z6FS1 7-way valve actuated using a stepper motor controlled from the data acquisition system. The test section dynamic pressure (pressure difference across the contraction) was also measured with the same transducer allowing for the following ventilated cavitation number to be derived in which the pressure transducer zero and span errors are eliminated (see also [13]).

$$\sigma_c = \frac{p_s - p_c}{\frac{1}{2}\rho U_\infty^2} = \frac{p_s - p_c}{K(p_2 - p_1)} \quad (1)$$

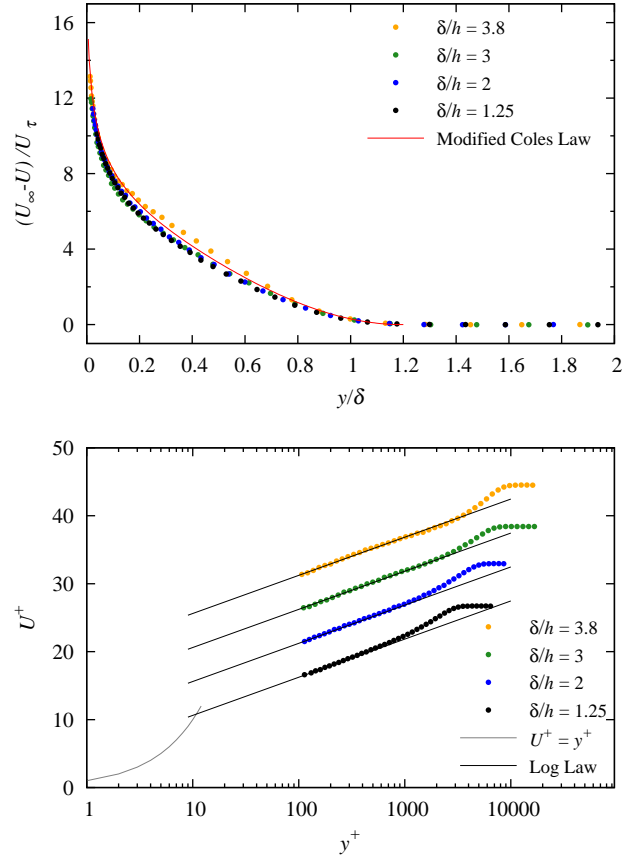


Figure 2. Boundary layer mean velocity profiles for the 4 boundary layers tested. The data is presented using both (top) outer variable scaling, and (bottom) inner variable scaling (the latter, plots staggered vertically by $U^+ = 5$).

where, p_c is the cavity pressure, p_s the freestream reference static pressure, U_∞ is the freestream reference velocity, ρ is the liquid density, K is the contraction constant and p_2 & p_1 are respectively, the static pressures upstream and downstream of the contraction.

All tests, including boundary layer measurements, were conducted at a constant Reynolds number, based on test section height, of 4×10^6 corresponding to a step height based Reynolds number of 66.7×10^3 . For the ventilated cavity measurements, the freestream cavitation number (i.e. with p_c exchanged for the liquid vapor pressure in equation 1) was kept at a constant value of 1.2.

Results and Discussion

Boundary layer profiles

Tests were conducted for a range of 4 boundary layer thicknesses, $1.25h \leq \delta \leq 3.8h$ (equating to momentum thickness Reynolds numbers from 8.5 to 28×10^3), which were obtained by thinning (1.25h), natural (2h), i.e. without using the boundary layer thickening system, and two thickened boundary layers (3 & 3.8h) achieved by differing flow rates. The measured profiles were of similar shape to those obtained in the bare test section without the plate fitted (see [1]) and so the plate leading edge is assumed have a negligible effect on the developing boundary layer. A modified Coles law equation, as used in the previous study, has also been plotted for comparison. Only the thicker of the two thickened boundary layers has had an insufficient development length to mix out fully, as was similarly found with some of the thickened boundary layers in the bare test section



Figure 3. Image of a ventilated cavity detaching from a BFS for $\delta/h = 2.0$ & $C_{Qv} = 0.027$. The 2-D nature of the cavity is apparent indicating that the ventilation flow is sufficiently distributed across the span of the step. The cavity closure is identifiable (indicated by the white dashed line) with air discharging from the closure region in shed cloud cavities and individual bubbles. Flow is from right to left.

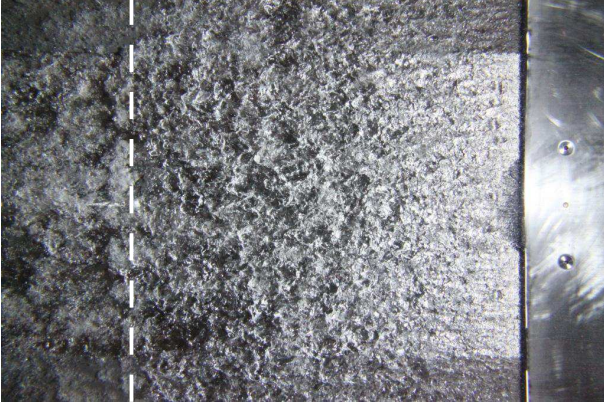


Figure 4. Image of a ventilated cavity detaching from a BFS for $\delta/h = 2.0$ & $C_{Qv} = 0.068$. With an increase in ventilation rate the cavity grows in length and the increase in gas discharge from the closure makes the length of the cavity less distinct (compare with figure 3).

[1], with a region in the wake having a slight excess in velocity defect when compared with the other three profiles. An improved plate geometry is currently under development.

Cavity length

As the cavity closure is inherently unsteady, a mean cavity length was determined for each flow condition from the average of ten images with the closure oscillating typically over a length of 20 to 50 mm. Typical images of a ventilated cavity ($\delta/h = 2$) are shown in figures 3 & 4, for the maximum and minimum ventilation rates, respectively. From the initial detachment from the step, the cavity surface has a wavy appearance attributable to the turbulence in the upstream boundary layer, with the amplitude of the disturbance growing with downstream distance, eventually contributing to the break up of the cavity. From a previous study on base-ventilated hydrofoils [13, 12], for some conditions the cavity surface was initially undisturbed (glassy appearance) attributable to a laminar boundary layer upstream of the step. Evaluation of the cavity length was undertaken by manual selection of the cavity closure position from the images and by image processing using intensity thresh-holding. The later was found to be quite sensitive to the selected threshold value as there was considerable variability in the pixel intensity with cavity length as the light positioning was limited due to the

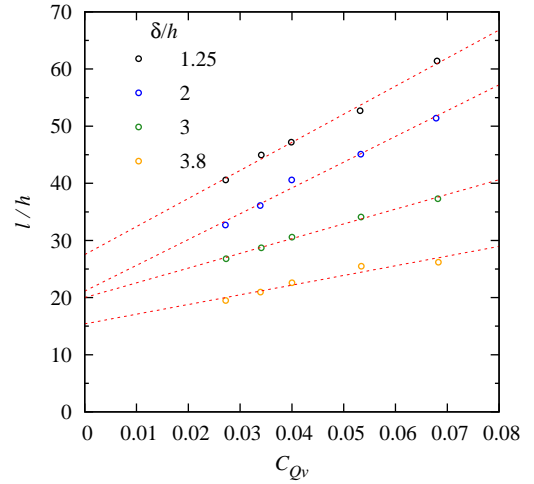


Figure 5. Cavity length versus ventilation rate for the 4 boundary layer thickness tested. The straight lines are linear least square fits through the experimental data indicating that the cavity length is linearly dependent on the ventilation rate.

available widow access. The manual procedure was chosen as the preferred method as this gave a more reliable measurement. For a future study, an improved arrangement for optical access will be used whereby a shadowgraph rather than a reflective lighting technique, can be employed for determining the cavity length.

The effect of ventilation rate and boundary layer thickness on cavity length is shown in figure 5. Cavity length increases linearly with ventilation rate and reduces with increase in boundary layer thickness. The latter effect is due to the reduced 'local' freestream velocity at the step outer edge due to the presence of the boundary layer. This consequently reduces the denominator in Eq. 1 resulting in an effectively lower cavitation number which implies a shorter cavity length. There is a difference in slope between the thinned and natural boundary layers ($\delta = 1.25h$ & $2h$) and the two thickened boundary layers which may be attributable to a difference in turbulence profiles as the mean velocity profiles, except for the thickness boundary layer, are virtually identical (figure 2). Turbulence profile measurements are planned, but have not been made for the present study.

Analytical modelling by Callenaere et al. [5] gives the following relationship for the cavity length of a (natural or vaporous) partial cavity formed off a BFS.

$$\frac{l}{h} = \frac{\lambda}{\pi} \left[\frac{(1-\lambda)^2}{\lambda^2} + \ln \frac{\lambda^2}{1-2\lambda+2\lambda^2} \right] \quad (2)$$

where $\lambda = \frac{1}{2} \left[1 - \frac{1}{\sqrt{1+\sigma_c}} \right]$ is the re-entrant jet thickness.

The present data compares reasonably with equation 2 but generally shows a reduced cavity length. This may be explained by both a difference in cavity physics, with the addition a ventilated flow interfering with the re-entrant jet formation and/or its flow back into the cavity, and also the lower 'local' freestream velocity effect due to the boundary layer presence as discussed above. There is a large scatter in the data, particular as $\sigma_c \rightarrow 0$, which occurs due to the numerator ($p_1 - p_c$) in equation 1 becoming small with respect to the denominator ($p_1 - p_2$). As the same transducer is used to measure both pressure differences, with the associated advantages as described above, in this instance it has resulted in a large error as $p_1 - p_c$ approaches zero. To overcome this limitation, it is planned to repeat the measurements

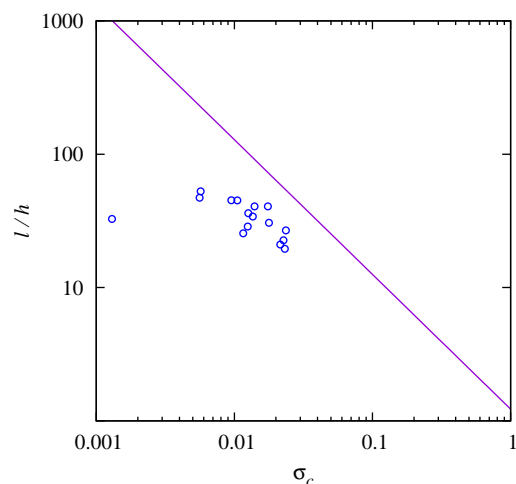


Figure 6. Cavity length as a function of the cavitation number. An analytical prediction [5] (see equation 2) for a naturally occurring cavity, i.e. from vapor only, is the straight solid line.

with separate transducers, having sensitivities appropriate to the disparate ranges involved.

Conclusions

The ventilated cavity flow over a BFS has been experimentally investigated as to the dependence of the cavity geometry on both the ventilation rate and upstream boundary layer thickness. The cavity length was found to increase linearly with ventilation rate and decreases with increased boundary layer thickness. The results obtained so far indicate that the dependence of cavity length on cavitation number for a ventilated cavity is similar to the natural cavity case but that there is reduction in length due to the different physics involved, i.e. the presence of the incompressible air and the upstream boundary layer. The dependence of the cavity geometry on the upstream boundary layer thickness has implications for the longitudinal location of the BFS on a vessel hull employing such a device for viscous drag reduction. Modifications to the experiment design have been identified which will allow for improved measurements to be obtained in a future follow on study.

Acknowledgements

The authors wish to acknowledge the assistance of Mr Robert Wrigley in carrying out the experiments and the support of the Australian Maritime College.

References

- [1] Brandner, P. A., Belle, A., Pearce, B. W. and Holmes, M. J., Artificial thickening of cavitation tunnel boundary layers, in *18th Australasian Fluid Mechanics Conference*, Paper 228, Launceston, Australia, 2012.
- [2] Brandner, P. A., Lecoffre, Y. and Walker, G. J., Development of an Australian national facility for cavitation research, in *Sixth International Symposium on Cavitation - CAV2006*, MARIN, Wageningen, The Netherlands, 2006.
- [3] Brandner, P. A., Lecoffre, Y. and Walker, G. J., Design considerations in the development of a modern cavitation tunnel, in *16th Australasian Fluid Mechanics Conference*, Gold Coast, Australia, 2007, 630–637.
- [4] Brice, R., *Ventilated super-cavitating flow past a backward facing step*, Research project, Australian Maritime College, 2006.
- [5] Callenaere, M., Franc, J.-P., Michel, J.-M. and Riondet, M., The cavitation instability induced by the development of a re-entrant jet, *Journal of Fluid Mechanics*, **444**, 2001, 223–256.
- [6] Ceccio, S. L., Friction drag reduction of external flows with bubble and gas injection, *Annual Review of Fluid Mechanics*, **42**, 2010, 183–203.
- [7] Elbing, B. R., Dowling, D. R., Perlin, M. and Ceccio, S. L., Diffusion of drag-reducing polymer solutions within a rough-walled turbulent boundary layer, *Physics of Fluids*, **22**, 2010, 045102.
- [8] Elbing, B. R., Mkiharju, S., Wiggins, A., Perlin, M., Dowling, D. R. and Ceccio, S. L., On the scaling of air layer drag reduction, *Journal of Fluid Mechanics*, **717**, 2013, 484–513.
- [9] Faltinsen, O. M., *Hydrodynamics of high-speed marine vehicles*, Cambridge University Press, Cambridge, Eng., 2005.
- [10] Lay, K. A., Yakushiji, R., Mkiharju, S., Perlin, M. and Ceccio, S. L., Partial cavity drag reduction at high Reynolds numbers, *Journal of Ship Research*, **54**, 2010, 109–119.
- [11] Mkiharju, S. A., Perlin, M. and Ceccio, S. L., On the energy economics of air lubrication drag reduction, *International Journal of Naval Architecture and Ocean Engineering*, **4**, 2012, 412–422.
- [12] Pearce, B. and Brandner, P., The effect of vapour cavitation occurrence on the hydrodynamic performance of an intercepted base-ventilated hydrofoil, in *18th Australasian Fluid Mechanics Conference*, Launceston, Australia, 2012, Paper 391.
- [13] Pearce, B. W. and Brandner, P. A., Experimental investigation of a base-ventilated supercavitating hydrofoil with interceptor, in *Eighth International Symposium on Cavitation - Cav2012*, Singapore, 2012, Paper No. 218.
- [14] Procaccia, I., Lvov, V. S. and Benzi, R., Colloquium: Theory of drag reduction by polymers in wall-bounded turbulence, *Reviews of Modern Physics*, **80**, 2008, 225–247.
- [15] Shiri, A., Leer-Andersen, M., Bensow, R. E. and Norrby, J., Hydrodynamics of a displacement air cavity ship, in *29th Symposium on Naval Hydrodynamics*, Gothenburg, Sweden, 2012.